

Numerical solution of the liquid film model for intermittent gas-liquid flows

Alysson H. R. de Almeida^{1,*}, Luiz E. M. Lima^{1,†}

¹*Department of Mechanics, Federal University of Technology — Paraná
330 Doutor Washington Subtil Chueire St., Jardim Carvalho, Ponta Grossa, PR 84017-220, Brazil
alysson.2018@alunos.utfpr.edu.br, †lelima@utfpr.edu.br

Abstract. Multiphase flows occur in several industrial sectors, such as oil and natural gas production and transport. Its understanding gives several technical and economic advantages. Gas-liquid flows are often grouped into three main patterns: dispersed, separated, and intermittent. A succession of liquid pistons (aerated or non-aerated) and elongated gas bubbles parallel with a thin liquid film that repeats itself over the pipe in a non-periodic way describes the intermittent or slug flow. These flows can occur in a steady state considering the unit cell concept. Thus, the hydrodynamic parameters of this kind of flow can be estimated using several models developed based on this concept. This work aims to solve numerically one of the models more complete for film profile estimation using a fourth-order Runge-Kutta method. A computational code is being written in MATLAB to implement the film profile model and the empirical correlations for estimating the closure parameters. The numerical results obtained for the film and piston lengths were compared with experimental data from the literature to validate the model solution employed. In addition, liquid film (or elongated gas bubble) profiles were plotted graphically for visualization and comparison with descriptions presented in the literature.

Keywords: two-phase flow, slug flow, modeling, numerical analysis.

1 Introduction

Multiphase flow is exhibited in diverse situations in nature and many processes, for example, combustion in engines, propulsion systems, fluids in the human body, nuclear power generation, transport of oil and gas, and food production, among others [1]. Thereby, methods to estimate its behavior are essential. Among the possible shapes that multiphase flow can show, three primary patterns appear when a gas-liquid mixture occurs: dispersed, separated, and intermittent. These patterns develop depending on the characteristics of the phases considered and their physical properties, the pipe geometrical properties (diameter, inclination, and roughness), and initial operating conditions, such as the flow rates of each phase. Among these shapes, the intermittent gas-liquid flow (slug flow) is present in various processes, as it is found in a broad set of gas and liquid flow rates. Therefore, there is an overall effort to develop a capable physical model that accurately represents its behavior, despite the dependence on empirical correlations [2].

Intermittent flow is characterized by liquid pistons (slugs), with or without dispersed gas bubbles (depending on operating conditions), followed by elongated gas bubbles containing a well-defined contact interface with a liquid film. Along the pipe is a repetition of this structure consequent from this pattern. Wallis [3] proposed an approach in which the intermittent flow regions constitute two distinct patterns: dispersed flow for the liquid slug and separate flow for the elongated gas bubble. Thus, the unit cell concept arises, assuming that this structure occurs as a phenomenon in steady-state, which is periodically repeated along the pipe, which resulted in the development of mathematical models that allowed an improved understanding of the dynamics in intermittent flow and its pertinent parameters.

Dukler and Hubbard [4] developed the first of these models, considering the flow to be one-dimensional and with negligible pressure drop along the elongated bubble length. Furthermore, the mass and *momentum* balances do not consider the gas phase influences. In this way, a free surface serves as a model for the film in the elongated bubble region.

Later, Gregory et al. [5] detected the need for a term that thoughtful the elongated bubble drift velocity relative to the film. This velocity significantly influences the model, making the hydrodynamic differences noticeable compared to an elongated bubble moving in stagnant liquid, especially in relatively wide pipes with slight inclinations. In addition, they related the velocity of the elongated bubble nose with the mixture superficial velocity.

Kokal and Stanislav [6] found the dependence of pressure drop on flow patterns in their work and presented an unprecedented model that considers the shear stress at the interface between an elongated bubble and its respective film. However, they did not feel the shear stress of the elongated bubble with the pipe wall. Their results exhibited satisfactory agreement with experimental data, mainly for higher gas flows, compared to preceding models, which did not consider the influence of interfacial shear stress.

These models had an extraordinary evolution in the work of Taitel and Barnea [7], which still stands today as a reference in finding results for intermittent flow. Their model developed is regarded as the most complete, serving as a basis for improvements proposed over the years since then; because, for the first time, the model considers the effects of the gas phase. These effects are present both in the elongated bubble, taking into account the shear stress of the bubble with the pipe wall, and in the liquid slug, where little dispersed bubbles may interact with the liquid phase, presenting velocity different from the same.

Trying to improve the Taitel and Barnea [7] model and the closure correlations, Andreussi et al. [8] highlighted that the presence of dispersed bubbles in the film is significant for air-water flows at high velocities and, possibly, more applicable for liquids with low surface tension. This phenomenon may be relevant in determining the average fraction of liquid present in a unit cell. Thus, they considered the presence of two distinct gas streams in their model, in the elongated bubble and another dispersed in the film.

Cook and Behnia [9] concluded in their work that the accuracy of the results, based on the model of Taitel and Barnea [7], heavily influences the choice of correlation for calculating the translational velocity of the elongated bubble. Considering this velocity is around 1.2 times the value of the mixture's superficial velocity, it becomes possible to obtain more consistent results. Furthermore, their model disregarded gravity's influence on the gas phase. They analyzed the pressure gradient separately for each phase so that the terms related to the buoyant force are functions of gas and liquid densities.

The work of Fagundes Netto et al. [10] contributed to a better understanding of the intermittent flow structure and its development along the pipe, achieved by examining the influence of the flow velocity and the bubble volume on its shape. They also proposed a model that considers the elongated bubble to consist of four parts: the nose, the body, the tail, and a hydraulic jump between the tail and the body. This hydraulic jump represents a rapid change in film thickness, causing a static pressure difference.

Cook and Behnia [11] proposed a reformulation of the Taitel and Barnea [7] model, adding a term due to the effective viscosity of the aerated liquid slug in the pressure drop calculation. Orell [12] found in their experimental study that this term is significant for high superficial velocities of the gas phase, especially for air-oil systems.

This work aims to compare the results obtained with the Taitel and Barnea [7] model against experimental data from the literature for the liquid film length. A computational code developed in MATLAB® in the present work performs the numerical integration of the model and the calculation of all related parameters.

2 Model

Considering an isothermal gas-liquid mixture (with known physical properties of the phases: density ρ , dynamic viscosity μ , and surface tension σ) flowing with volumetric flow rate Q in a pipe of length L , diameter D , perimeter S , area A , and inclination θ , the unit cell has a length L_U , resulting from the sum of L_F and L_S , which represent the lengths of the film and the slug, respectively. Figure 1 shows a representation of this flow pattern.

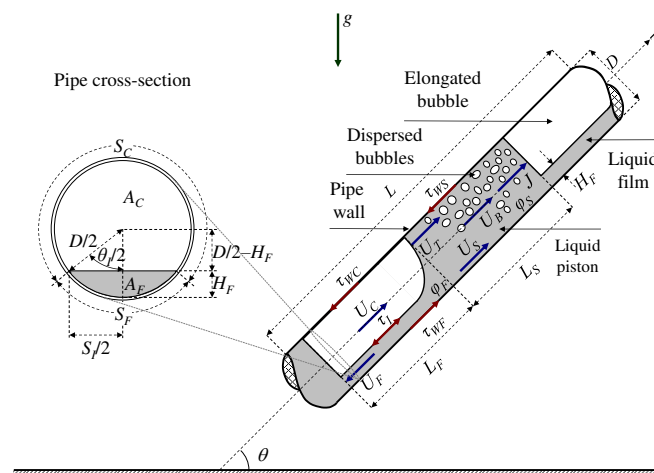


Figure 1. Representation of the model and its variables [13].

The physical modeling employs the unit cell model proposed by Taitel and Barnea [7], based on the discussion given by Shoham [2]. Taitel and Barnea [7] sought to unify a model applicable to flows in pipes with any inclination, proposing three approaches studying film hydrodynamics, two of which assume simplifying hypotheses. The first takes an equilibrium and constant film thickness along the region of the elongated bubble and the film: $H_F \equiv H_{Fe} = \text{constant}$ and $-(dp/dz) \neq 0$. The second assumes a free surface open-channel flow for the film: $H_F \neq \text{constant}$ and $-(dp/dz) = 0$. The third presents a more precise description that requires the numerical solution of a more detailed equation to estimate the film profile, with $H_F \neq \text{constant}$ and $-(dp/dz) \neq 0$, which is the approach used in the present work and defined by Eq. (1):

$$\frac{dH_F}{dz_F} = \frac{\frac{\tau_{WF}S_F}{A_F} - \frac{\tau_{WC}S_C}{A_C} - \tau_I S_I \left(\frac{1}{A_F} + \frac{1}{A_C} \right) + (\rho_L - \rho_G) g \sin \theta}{(\rho_L - \rho_G) g \cos \theta - \left[\rho_L \frac{(U_T - U_F)^2}{\phi_F} + \rho_G \frac{(U_T - U_C)^2}{1 - \phi_F} \right] \frac{S_I}{A}} \quad (1)$$

From the numerical integration procedure of Eq. (1), shown in Section 2.1, the liquid phase mass balance in Eq. (2) must be satisfied to obtain the length of the film L_F (or the elongated bubble).

$$J_L = U_S \phi_S + f \left[(1 - \phi_S) L_F - \int_0^{L_F} (1 - \phi_F) dz_F \right] \quad (2)$$

Where the liquid superficial velocity is $J_L (\equiv Q_L/A)$, just as the gas superficial velocity is $J_G (\equiv Q_G/A)$.

Carvalho and Lima [14] analyzed the accuracy of various empirical correlations against experimental data of unit cell frequency $f (\equiv U_T/L_U)$, and one of the best was that of Fossa et al. [15], defined in Eq. (3):

$$f = \frac{J_G}{D} \left(\frac{0.044 \lambda_L}{1 - 1.71 \lambda_L + 0.70 \lambda_L^2} \right) \quad (3)$$

Where $\lambda_L (= J_L/J)$ is the homogeneous liquid holdup (fraction).

The shear stresses of the phases with the pipe walls must be expressed using the local velocities of the phases, according to Eqs. (4) and (5). On the other hand, the interfacial shear stress considers the relative velocity between the phases, according to Eq. (6).

$$\tau_{WF} = \frac{1}{2} C_{fF} \rho_L |U_F| U_F \quad (4)$$

$$\tau_{WC} = \frac{1}{2} C_{fC} \rho_G |U_C| U_C \quad (5)$$

$$\tau_I = \frac{1}{2} C_{fI} \rho_G |U_C - U_F| (U_C - U_F) \quad (6)$$

The Blasius correlation for hydraulically smooth pipes can be employed to determine the friction factors (Fanning) of the phases, defined in Eqs. (7) and (8) (with: $m = 16$ and $n = 1$ if laminar; $m = 0.046$ and $n = 0.2$ if turbulent); but for rough pipes, there are several other correlations in the literature for this. The interfacial friction factor can be estimated using Eq. (9), which may depend on the dimensionless film thickness $\delta_F (\equiv H_F/D)$.

$$C_{fF} = m \left(\frac{U_F D_F \rho_L}{\mu_L} \right)^{-n} \quad (7)$$

$$C_{fC} = m \left(\frac{U_C D_G \rho_G}{\mu_G} \right)^{-n} \quad (8)$$

$$C_{fI} = \begin{cases} 0.014 & \text{if flat film [16, 17]} \\ 0.005 (1 + 300 \delta_F) & \text{if concentric film [3]} \end{cases} \quad (9)$$

The kinematic law proposed by Nicklin [18] adequately models the translational velocities of the elongated bubble U_T and the bubbles dispersed in the liquid slug U_B as a function of the mixture superficial velocity $J (\equiv J_L + J_G)$, according to Eqs. (10) and (11), respectively:

$$U_T = C_{0T}J + V_{\infty T} \equiv C_{0T}J + Fr_{\infty T} \sqrt{gD(1 - \rho_G/\rho_L)} \quad (10)$$

$$U_B = C_{0B}J + V_{\infty B} \equiv C_{0B}J + Fr_{\infty B} \sqrt{gD(1 - \rho_G/\rho_L)} \quad (11)$$

Table 1 presents the definitions for the distribution parameters, C_{0T} and C_{0B} , and the drift Froude numbers, $Fr_{\infty T}$ and $Fr_{\infty B}$, of the elongated bubble [19, 20] and the dispersed bubbles [21], presented in Eqs. (10) and (11), as a function of the Eötvös and Froude numbers for the mixture, defined as $Eo = gD^2(\rho_L - \rho_G)/\sigma$ and $Fr = J/\sqrt{gD(1 - \rho_G/\rho_L)}$, respectively.

Table 1. Definitions for distribution parameters and drift Froude numbers considering turbulent flow [13].

| Bubble(s) | k | C_{0k} | $Fr_{\infty k}$ | Criterion |
|-----------|-----|-------------------------|--|---------------|
| Elongated | T | $1 + 0.2 \sin^2 \theta$ | $(0.542 - \frac{1.76}{Eo^{0.56}}) \cos \theta + \frac{0.345 \sin \theta}{(1+3805Eo^{-3.06})^{0.58}}$ | $Fr < 3.5$ |
| | | 1.2 | $\frac{0.345 \sin \theta}{(1+3805Eo^{-3.06})^{0.58}}$ | $Fr \geq 3.5$ |
| Dispersed | B | $1 + 0.2 \sin^2 \theta$ | $1.54Eo^{-1/4} \phi_S^{7/4} \sin \theta$ | – |

Mass balances and definitions of relative velocities provide expressions for the average velocities of liquid in the slug, film, and gas in the elongated bubble, according to Eqs. (12) to (14), respectively:

$$U_S = \frac{J - U_B(1 - \phi_S)}{\phi_S} \quad (12)$$

$$U_F = U_T - \frac{(U_T - U_S)\phi_S}{\phi_F} \quad (13)$$

$$U_C = \frac{J - U_F\phi_F}{1 - \phi_F} \quad (14)$$

Barboza et al. [22] analyzed the accuracy of various empirical correlations against experimental data of slug liquid holdup ϕ_S , and one of the best was that of Xu [23], defined in Eq. (15):

$$\phi_S = \left[1 + \left(\frac{J}{9.514} \right)^{1.274} \right]^{-1} \quad (15)$$

The film holdup ϕ_F (liquid fraction in the elongated bubble region) is defined from the geometrical relations of the interfaces. As well as perimeters S_k , areas A_k , and hydraulic diameters D_k of the phases or regions k ($= G, F, I$), according to Tab. 2. These geometrical properties are functions of the angle resulting from the flat interface, defined as $\theta_I = 2 \arccos(1 - 2\delta_F)$, or directly in terms of the dimensionless film thickness δ_F , for a concentric interface.

Table 2. Geometrical properties of interfaces [13].

| Geometrical properties | Interface | |
|------------------------|---|---------------------------------|
| | Flat | Concentric |
| S_C | $D(\pi - \theta_I/2)$ | 0 |
| S_F | $D\theta_I/2$ | πD |
| S_I | $D \sin(\theta_I/2)$ | $\pi D(1 - 2\delta_F)$ |
| A_C | $D^2(2\pi - \theta_I + \sin \theta_I)/8$ | $\pi D^2(1 - 2\delta_F)^2/4$ |
| A_F | $D^2(\theta_I - \sin \theta_I)/8$ | $\pi D^2\delta_F(1 - \delta_F)$ |
| D_G | $D \left[1 + \frac{\sin(\theta_I/2) - \sin \theta_I/2}{2(2\pi - \theta_I + \sin \theta_I)} \right]^{-1}$ | $D(1 - 2\delta_F)$ |
| D_F | $D(1 - \sin \theta_I/\theta_I)$ | $D[4\delta_F(1 - \delta_F)]$ |
| ϕ_F | $(\theta_I - \sin \theta_I)/(2\pi)$ | $4\delta_F(1 - \delta_F)$ |

2.1 Numerical solution procedure

In Equation (1), all terms vary along the axial coordinate z_F . Still, the physical properties of the fluids and the pipe characteristics are constant at each integration step i , as well as the cell frequency and the slug holdup. The integration process of Eq. (1) to obtain the profile of the film thickness, $H_F = H_F(z_F)$, was performed using the fourth-order Runge–Kutta method, and together with the model equation, auxiliary equations, and empirical correlations were implemented in a computational code developed in MATLAB[®]. The integration starts at the bubble nose and marches along its length until Eq. (2) is satisfied; consequently, the total film length, L_F , is reached. Shoham [2] suggests $H_{F0} \approx \phi_S D$ as the initial condition for the film thickness, i.e., the initial film holdup ϕ_F is equal to the average slug holdup ϕ_S in front of this film. The definition of the initial value problem corresponds:

$$\frac{dz_F}{dH_F} = F(H_F, z_F), \quad z_F(H_{F0}) = 0 \quad (16)$$

Moreover, as the bubble lies on the pipe upper part, H_F always diminishes as z_F distance increases until it reaches an equilibrium value H_{Fe} , i.e., $(dH_F/dz_F) \rightarrow 0$. Unfortunately, some flow conditions result in $(dH_F/dz_F) > 0$, which is discrepant with the physical evidence. Still, it must be related to the inflection point at the bubble nose, as seen in Fig. 1. To define H_{F0} for these flow conditions, it has to be decreased gradually until $(dH_F/dz_F) < 0$ are encountered [7, 9, 10]. Using a step-size $\Delta H_F > 0$, such that $H_{F,i+1} = H_{F,i} - \Delta H_F$, and it is calculated:

$$z_{F,i+1} = z_{F,i} - \frac{\Delta H_F}{6} [k_1 + 2(k_2 + k_3) + k_4], \quad \begin{cases} k_1 = F(H_{F,i}, z_{F,i}) \\ k_2 = F(H_{F,i} - \frac{\Delta H_F}{2}, z_{F,i} - k_1 \frac{\Delta H_F}{2}) \\ k_3 = F(H_{F,i} - \frac{\Delta H_F}{2}, z_{F,i} - k_2 \frac{\Delta H_F}{2}) \\ k_4 = F(H_{F,i} - \Delta H_F, z_{F,i} - k_3 \Delta H_F) \end{cases} \quad (17)$$

3 Analysis method

The determination of the relative deviation modulus ϵ_R between the calculated and measured values for the dimensionless film length L_F/D is the base of the accuracy analysis of the unit cell model. Also, this analysis considers the RMS (Root Mean Square) values of the relative deviations referring to the total number of experimental tests. The experimental data used in this work comes from other work found in the literature. Bueno [24] conducted ten experiments using air and water as a mixture in a horizontal test section of $306D$ length and 26 mm inner diameter. The experimental apparatus consists of the flow in two separate circuits of air and water carried to a mixer to constitute the two-phase flow. After, it passes through the acrylic test section, where two different stations measure the data downstream of the mixer, one $77D$ and another $257D$. At these stations, impedance sensors monitor the intermittent flow data, and a data acquisition system obtains and processes the data. After going through the test section, a vertical pipe of 75 mm inner diameter acts as an air and water separator for the mixture discharged into this pipe. Table 3 presents the intervals of the variables determined in the experiments by Bueno [24].

Table 3. Variables intervals of the experimental dataset of the Bueno [24].

| J_G / (cm/s) | J_L / (cm/s) | J_G/J_L | λ_L | P / (mbar) | L_F/D | N |
|----------------|----------------|-----------|-------------|--------------|-----------|-----|
| 30.2–142.1 | 29.0–121.0 | 0.47–4.90 | 0.17–0.68 | 982–1058 | 7.5–140.2 | 10 |

The properties of the fluids are necessary to start the numerical integration of the unit cell model come from literature, considering the operational conditions of the Bueno [24] experiments: atmospheric pressure of $P_{atm} = 947$ mbar and ambient temperature $T = 25$ °C. The ideal gas state equation estimates the air density, considering this ambient temperature and the local absolute pressure at each experimental test.

4 Results and discussion

Figure 2 shows the profiles of the dimensionless liquid thickness δ_F as a function of the non-dimensional axial coordinate z_F/D for each test condition of the Bueno [24] experimental dataset. Each profile in Fig. 2 corresponds to a homogeneous liquid holdup λ_L of all tests of the Bueno [24] experimental dataset. Five tests with $\lambda_L < 0.5$ (Fig. 2a) and five tests with $\lambda_L \geq 0.5$ (Fig. 2b). These λ_L values are the result of distinct combinations of gas and liquid superficial velocity values, although some are very close.

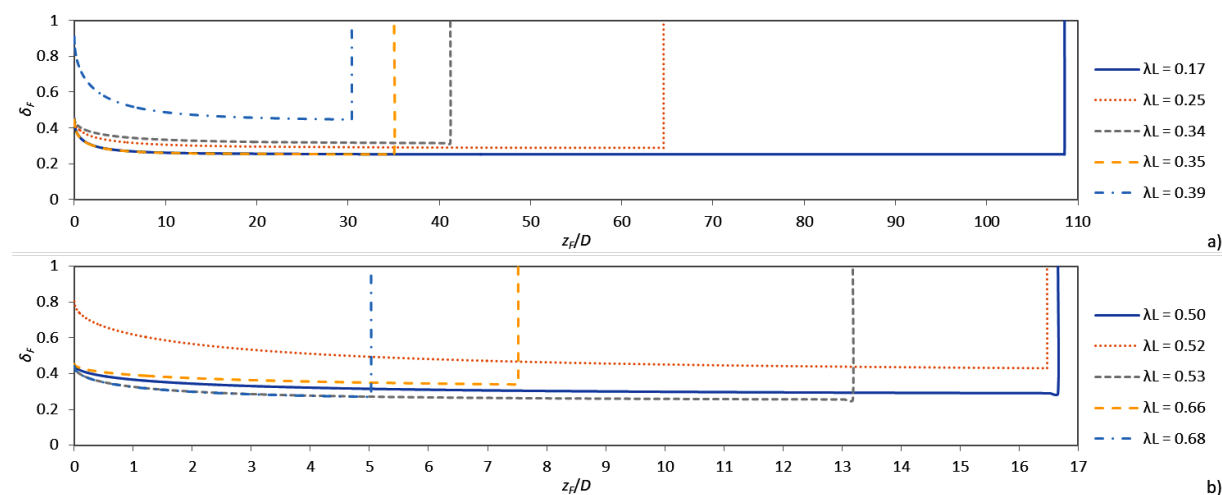


Figure 2. Profiles of the dimensionless liquid thickness as a function of the non-dimensional axial coordinate: a) $\lambda_L < 0.5$; b) $\lambda_L \geq 0.5$.

Figure 2 demonstrates that the dimensionless film length L_F/D decreases with the increase of the homogeneous liquid holdup λ_L , as expected from both theory and literature. In addition to λ_L , the dimensionless film thickness δ_F strongly depends on the gas-liquid ratio J_G/J_L , defining the film profile. Table 4 shows the relative deviation modulus ϵ_R between the calculated and measured values for the dimensionless film length L_F/D . The RMS value of the relative deviations was 14.08%, considering all data.

Table 4. Relative deviation modulus between the calculated and measured values for the dimensionless film length.

| λ_L | 0.17 | 0.25 | 0.34 | 0.35 | 0.39 | 0.50 | 0.52 | 0.53 | 0.66 | 0.68 |
|---------------------|-------|------|------|------|-------|------|------|------|------|-------|
| $\epsilon_R / (\%)$ | 22.60 | 4.34 | 1.76 | 0.70 | 10.77 | 6.00 | 3.01 | 5.37 | 0.66 | 35.47 |

Moreover, the model integration problem in the bubble nose region, described in Section 2.1, is highlighted, resulting in relatively small initial film thicknesses depending on the gas-liquid ratio, which also influences the film length and thickness along the bubble body.

5 Conclusions

This work presents a numerical solution of the film profile model for intermittent gas-liquid flows, using the unit cell model proposed by Taitel and Barnea [7]. The Fossa et al. [15] correlation for the cell frequency with the correlation Xu [23] for the slug holdup presents satisfactory results in the model integration procedure compared with the experimental data.

This analysis verified that the length and thickness of the film depend on the homogenous liquid holdup and gas-liquid ratio, demonstrating that the model results agree with both theory and literature. Therefore, all bubble shapes also vary according to these parameters, but the initial condition of the film thickness significantly influences the bubble nose shape; consequently, the film length as a result of the mass balance employed to finish the integration procedure of the model.

Future works can improve the modeling and integration process to solve the bubble nose region with better precision. Also, to analyze the influence of other closure parameters in the model and the employment of severe conditions can be realized.

Acknowledgements. This study was financed in part by the Fundação Araucária — Brasil (Public Notice UTFPR/PROPPG n.º 02/2021). The authors also thank the Federal University of Technology — Paraná.

Authorship statement. The authors hereby confirm that they are the sole liable persons responsible for the authorship of this work, and that all material that has been herein included as part of the present paper is either the property (and authorship) of the authors, or has the permission of the owners to be included here.

References

- [1] N. I. Kolev. *Multiphase flow dynamics*. Springer, Berlin, Germany; New York, NY, USA, 2 edition, 2005.
- [2] O. Shoham. *Mechanistic modeling of gas-liquid two-phase flow in pipes*. Society of Petroleum Engineers (SPE), Richardson, TX, USA, 1 edition, 2006.
- [3] G. B. Wallis. *One-dimensional two-phase flow*. McGraw-Hill, New York, NY, USA, 1 edition, 1969.
- [4] A. E. Dukler and M. G. Hubbard. A model for gas-liquid slug flow in horizontal and near horizontal tubes. *Ind. Eng. Chem. Fundam.*, vol. 14, n. 4, pp. 337–347, 1975.
- [5] G. A. Gregory, M. K. Nicholson, and K. Aziz. Correlation of the liquid volume fraction in the slug for horizontal gas-liquid slug flow. *Int. J. Multiph. Flow*, vol. 4, n. 1, pp. 33–39, 1978.
- [6] S. L. Kokal and J. F. Stanislav. An experimental study of two-phase flow in slightly inclined pipes—II. Liquid holdup and pressure drop. *Chem. Eng. Sci.*, vol. 44, n. 3, pp. 681–693, 1989.
- [7] Y. Taitel and D. Barnea. Two-phase slug flow. In J. P. Hartnett and T. F. Irvine Jr., eds, *Advances in Heat Transfer*, volume 20, pp. 83–132. Elsevier, 1990.
- [8] P. Andreussi, K. H. Bendiksen, and O. J. Nydal. Void distribution in slug flow. *Int. J. Multiph. Flow*, vol. 19, n. 5, pp. 817–828, 1993.
- [9] M. Cook and M. Behnia. Film profiles behind liquid slugs in gas-liquid pipe flow. *AIChE J.*, vol. 43, n. 9, pp. 2180–2186, 1997.
- [10] J. R. Fagundes Netto, J. Fabre, and L. Peresson. Shape of long bubbles in horizontal slug flow. *Int. J. Multiph. Flow*, vol. 25, n. 6-7, pp. 1129–1160, 1999.
- [11] M. Cook and M. Behnia. Pressure drop calculation and modelling of inclined intermittent gas-liquid flow. *Chem. Eng. Sci.*, vol. 55, n. 20, pp. 4699–4708, 2000.
- [12] A. Orell. Experimental validation of a simple model for gas-liquid slug flow in horizontal pipes. *Chem. Eng. Sci.*, vol. 60, n. 5, pp. 1371–1381, 2005.
- [13] L. E. M. Lima. *Análise do modelo de mistura aplicado em escoamentos isotérmicos gás-líquido [Analysis of mixture model applied in gas-liquid isothermals flows]*. PhD thesis, Faculty of Mechanical Engineering (FEM), State University of Campinas (Unicamp), Campinas, SP, Brazil, 2011.
- [14] G. L. Carvalho and L. E. M. Lima. A review of frequency correlations for the intermittent gas-liquid flow in horizontal pipes. In *Proceedings of the 17th Brazilian Congress of Thermal Sciences and Engineering (ENCIT)*, pp. 251:1–251:10, Rio de Janeiro, RJ, Brazil. Brazilian Association of Engineering and Mechanical Sciences (ABCM), 2018.
- [15] M. Fossa, G. Guglielmini, and A. Marchitto. Intermittent flow parameters from void fraction analysis. *Flow Meas. Instrum.*, vol. 14, n. 4, pp. 161–168, 2003.
- [16] L. S. Cohen and T. J. Hanratty. Effect of waves at a gas-liquid interface on a turbulent air flow. *J. Fluid Mech.*, vol. 31, n. 3, pp. 467–479, 1968.
- [17] O. Shoham and Y. Taitel. Stratified turbulent-turbulent gas-liquid flow in horizontal and inclined pipes. *AIChE J.*, vol. 30, n. 3, pp. 377–385, 1984.
- [18] D. J. Nicklin. Two-phase bubble flow. *Chem. Eng. Sci.*, vol. 17, n. 9, pp. 693–702, 1962.
- [19] K. H. Bendiksen. An experimental investigation of the motion of long bubbles in inclined tubes. *Int. J. Multiph. Flow*, vol. 10, n. 4, pp. 467–483, 1984.
- [20] M. E. Weber. Drift in intermittent two-phase flow in horizontal pipes. *Can. J. Chem. Eng.*, vol. 59, n. 3, pp. 398–399, 1981.
- [21] T. Z. Harmathy. Velocity of large drops and bubbles in media of infinite or restricted extent. *AIChE J.*, vol. 6, n. 2, pp. 281–288, 1960.
- [22] G. F. Barboza, P. L. O. Machado, and L. E. M. Lima. Correlations review for the slug liquid holdup prediction in intermittent gas-liquid flows. In *Proceedings of the 18th Brazilian Congress of Thermal Sciences and Engineering (ENCIT)*, pp. 346:1–346:9, Rio de Janeiro, RJ, Brazil. Brazilian Association of Engineering and Mechanical Sciences (ABCM), 2020.
- [23] J.-y. Xu. A simple correlation for prediction of the liquid slug holdup in gas/non-Newtonian fluids: horizontal to upward inclined flow. *Exp. Therm. Fluid Sci.*, vol. 44, pp. 893–896, 2013.
- [24] L. G. G. Bueno. Estudo experimental de escoamentos líquido-gás intermitentes em tubulações inclinadas [experimental analysis of slug flow in inclined lines]. Master's thesis, Faculty of Mechanical Engineering (FEM), State University of Campinas (Unicamp), Campinas, SP, Brazil, 2010.